phys. stat. sol. (a) **205**, No. 12, 2737–2751 (2008) / **DOI** 10.1002/pssa.200880458

physica status solidi a
www.pss-a.com
applications and materials science

Detailed balance and reciprocity in solar cells

Thomas Kirchartz* **and Uwe Rau****

IEF5-Photovoltaik, Forschungszentrum Jülich, 52425 Jülich, Germany

Received 10 July 2008, revised 7 October 2008, accepted 9 October 2008
Published online 18 November 2008

PACS 72.40.+w, 78.60.Fi, 84.60.Bk, 84.60.Jt, 85.60.Bt, 85.60.Jb

* Corresponding author: e-mail t.kirchartz@fz-juelich.de, Phone: +00 49 2461 613932
** e-mail u.rau@fz-juelich.de, Phone: +00 49 2461 611544

The limiting efficiency of photovoltaic devices follows from the detailed balance of absorption and emission of a diode according to the Shockley–Queisser theory. However, the principle of detailed balance has more implications for the understanding of photovoltaic devices than only defining the efficiency limit. We show how reciprocity relations between carrier collection and dark carrier injection, between electroluminescence emission and photovoltaic quantum efficiency and between open circuit voltage and light emitting diode quantum efficiency all follow from the principle of detailed balance. We also discuss the validity range of the Shockley–Queisser limit and the reciprocity relations. Discussing the validity of the reciprocity relations helps to deepen the understanding of photovoltaic devices and allows us to identify interrelationships between the superposition principle, the diode ideality and the reciprocity relations.

1 Introduction The field of photovoltaics has seen two remarkable developments within the last years. The first is that it has become a rapidly growing business with crystalline silicon as the predominant technology and inorganic thin film approaches as promising alternatives [1]. The second development is that research has expanded [2, 3] from p–n-junction type silicon solar cells to completely different materials and working principles of the photovoltaic device like organic [4–12] or dye sensitized [13–17] solar cells. The evolutionary process of solar cell research leading to state-of-the-art solar cells had economic success while creating a wish for revolutionary progress in research. No longer are only those technologies pursued that seem to work nearly immediately. Instead, theoretical concepts are sought after and materials and devices are designed [18] that may provide the basis for future solar cell generations.

Initial efficiencies of many devices using new concepts are rather low while the number of scientific disciplines involved and the number of scientific aspects to be considered is fairly high. More generally speaking, the number of models describing a given device is inversely proportional to its efficiency. The perfect device is described by one model, a good device by few modifications and a bad device needs a lot of explanations why it does not perform properly. This is because there is virtually an infinite number of possible reasons why a thing does not work. This article does not intend to add another model for any specific solar cell. Instead we aim at the basic understanding of *all* photovoltaic devices and at principles that must be common for everything between actual industrial solar modules and innovative concepts for future solar cells.

The logical starting point is the situation, when only one theory is necessary. The efficiency limit of any single bandgap solar cell was derived by Shockley and Queisser [19] from the detailed balance of absorbed and emitted radiation. The importance of the Shockley–Queisser (SQ) limit is twofold. For the current crystalline Si solar cell technology it constitutes an upper limit that is rather close to the efficiencies that have already been achieved [20]. For many approaches in research, however, it is not the limit up to which one can improve but the limit which is to be overcome. Thus, the assumptions underlying this limit and the possibilites under which they can be circumvented are of major interest for all high efficiency concepts.

2 The Shockley–Queisser limit To derive the maximum efficiency and the current/voltage (J/V)-curve of an idealized solar cell, only few assumptions have to be made. The basic ingredients to calculate this limit are the

detailed balance principle and Planck's law. The assumptions defining a cell in the SQ-limit are (i) perfect absorption of photons with energy E larger than a threshold energy (usually the band gap energy E_g) with each photon creating exactly one electron/hole pair, (ii) perfect collection of carriers – i.e. infinite mobility – and (iii) radiative recombination as the only allowed recombination mechanism. The only properties to describe the idealized SQ-cell are its bandgap and its temperature. The bandgap E_g defines the threshold for absorption of light, which is assumed to be perfectly abrupt, i.e. no light is absorbed below the bandgap and every photon is absorbed above the bandgap. The photogenerated current density J_{sc} under illumination with the photon flux ϕ_{sun} is therefore

$$J_{sc} = q\int_0^\infty a(E)\,\phi_{sun}(E)\,\mathrm{d}E = q\int_{E_g}^\infty \phi_{sun}(E)\,\mathrm{d}E\,, \tag{1}$$

where q is the elementary charge. Note that the second equality in Eq. (1) is obtained by assuming the absorptance $a(E)$ being a step-function which is zero below and unity above the bandgap energy E_g. Figure 1a illustrates this situation. Absorptance multiplied with the spectrum gives the photocurrent (hatched region) in the idealized cell.

In thermodynamic equilibrium, every process within the solar cell has to be in equilibrium with its inverse process. A violation of this law – the detailed balance principle – would cause a net flux of energy, which contradicts the assumption of thermodynamic equilibrium. From detailed balance of the radiative microscopic processes follows that the macroscopically observable photon fluxes in and out of a device are equal in equilibrium. The amount of black body radiation that is absorbed equals the amount that is emitted if environment and device have the same temperature. Hence, Kirchhoff's law follows, equating absorptance and emissivity of a body as a function of energy and angle.

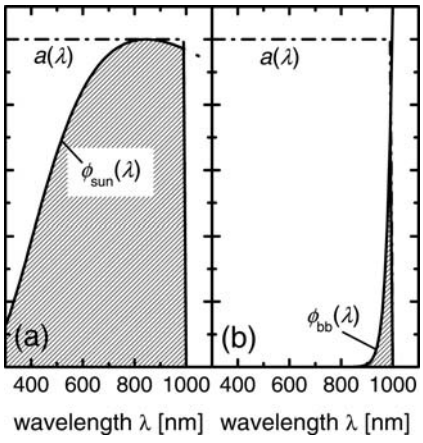

Figure 1 Photon flux that is (a) absorbed and (b) emitted by a solar cell with a step function like absorptance $a(E)$ and a perfect collection. The scale for the photon emission (b) depends on the applied voltage. The open circuit voltage in the SQ-limit is the voltage where the hatched regions are equal.

Planck's law [21] allowed the description of thermal radiation emitted by a black body with the temperature T. Non-thermal radiation, as encountered in a semiconductor under non-equilibrium, is described with a generalization of Planck's law that was introduced by Würfel. Non-equilibrium radiation is accounted for by a non-zero chemical potential of radiation μ_γ which is equal to the quasi-Fermi-level splitting at the position where radiation is emitted. Würfel's generalized Planck law [22] together with Kirchhoff's law [23] allows the calculation of the emission of an ideal diode with flat quasi-Fermi levels. The emitted photon flux ϕ under the applied bias voltage V is

$$\phi(V,E) = \frac{2\pi E^2}{h^3c^2}\,\frac{a(E)}{[\exp((E-qV)/kT)-1]}\,, \tag{2}$$

where h is the Planck constant, c the velocity of light in vacuum, $a(E)$ is the absorptance and emissivity of the solar cell, and kT is the thermal energy. For voltages that are small compared with the emitted photon energies, i.e. $E - qV \gg kT$, the Bose–Einstein term in Eq. (2) is well approximated by a Boltzmann distribution and we can simplify Eq. (2) to

$$\phi(V,E) = a(E)\,\phi_{bb}\,\exp(qV/kT)\,, \tag{3}$$

where the black body spectrum is defined by

$$\phi_{bb} = \frac{2\pi E^2}{h^3c^2}\exp\left(-\frac{E}{kT}\right). \tag{4}$$

The emission described by Eq. (2) must be caused by a recombination current J_{rec}. Since in the radiative limit, there are no other possibilities to recombine, the whole recombination current must be $J_{rec} = q\Phi$, where Φ denotes the integration of ϕ over energy. In thermodynamic equilibrium, the total current must be zero. Thus, the recombination current has to be the same as the photocurrent, caused by absorption of the black body radiation of the environment. In this situation, the total current is $J = q(\Phi(V=0) - \Phi(V=0)) = 0$. Under applied bias voltage in the dark and in the Boltzmann approximation, the total current is $J = q\Phi(0)\,(\exp(qV/kT)-1)$. The prefactor for the dark current is the radiative saturation current density

$$J_{0,rad} = q\Phi(0) = \int a(E)\,\phi_{bb}\,\mathrm{d}E = \int_{E_g}^\infty \phi_{bb}\,\mathrm{d}E\,. \tag{5}$$

Again the second equality is obtained by a step-function – like absorptance function $a(E)$. Though not considered in the original paper [19], the more general case of an arbitrary function $0 \le a(E) \le 1$ in Eqs. (1) and (5) is used for calculations of the radiative efficiency limit for real photovoltaic materials like Si [24] or for materials with lateral band gap fluctuations [25]. In the following, we will refer to the more general situation, i.e. the first integrals in Eqs. (1) and (5).

Under voltage bias and illumination, we have to subtract the short circuit current density and finally get

$$J = J_{0,\mathrm{rad}}(\exp(qV/kT) - 1) - J_{\mathrm{sc}} \,. \tag{6}$$

The SQ-theory produces an exponential current/voltage-curve that is mathematically already very close to the one of actual solar cells. Except for the inclusion of series- and parallel resistances, the major differences are the inclusion of non-radiative saturation current densities and of a diode quality factor n_{id} accounting for small deviations from the exponential slope of q/kT. The maximum attainable voltage is given by the voltage, where the solar cell emits as many photons as it absorbs. No net current flows implying that the solar cell is in open circuit conditions. The maximum voltage is therefore usually referred to as the open circuit voltage, which results from Eq. (6) by setting the total current $J = 0$ and solving for V, as

$$V_{\mathrm{oc}} = kT/q \,\ln(J_{\mathrm{sc}}/J_{0,\mathrm{rad}} + 1) \,. \tag{7}$$

The efficiency η of the solar cell follows directly from

$$\eta = \frac{\max(-JV)}{P_{\mathrm{opt}}} = \frac{J_{\mathrm{sc}} V_{\mathrm{oc}} FF}{P_{\mathrm{opt}}} \,, \tag{8}$$

where FF is the fill factor, P_{opt} is the optical power density of the incoming radiation and with the current as defined by Eq. (6). For an unconcentrated AM1.5G spectrum, the maximum efficiency is around 33%. The influence of the bandgap is rather weak in the range 1 eV < E_{g} < 1.45 eV, while for higher bandgaps the amount of unabsorbed low energy photons becomes too high. For lower band gaps, the photocurrent increases but the lower energy per electron/hole pair leads to a net decrease in both open circuit voltage and efficiency.

3 The principle of detailed balance

3.1 Discrete solar cell model The SQ-limit derives the maximum solar cell efficiency from macroscopic quantities of the solar cell, namely the absorptance and the temperature. The fundamental principle behind the SQ-limit, however, is a microscopic relation: the principle of detailed balance.

In the following, we will therefore discuss the principle of detailed balance in more detail. To illustrate the implications of the principle of detailed balance for the fundamental understanding of solar cells, it is most instructive to consider a discrete model first. This model might be the discretization of a continuous transport equation as used when solving the transport equation numerically but also the physically correct model for transport if essentially localized states are involved. The derivation starts with a similar argumentation as in Ref. [26] but includes the issue of photon emission. Thus, we also show the implications of the detailed balance on the relation between luminescent emission and absorption.

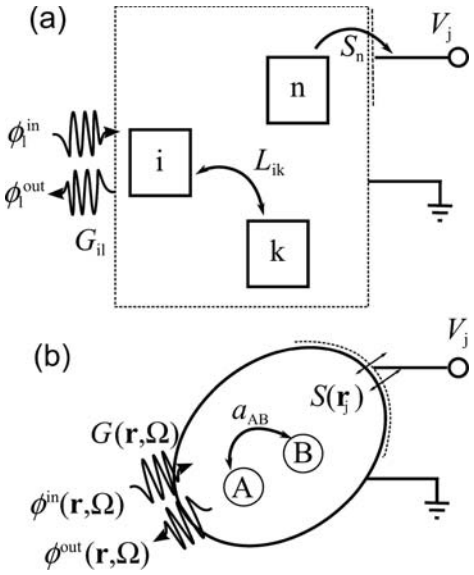

Figure 2 Scheme of the (a) discrete and (b) continuous solar cell model used for the direct derivation of the reciprocity from detailed balance.

Figure 2a shows the scheme of the discrete device model. At each site *i, k* or *n* in the absorber, we define a concentration of minority carriers. Minority carriers can be generated and emitted optically and they can be injected and extracted via the minority carrier contact.

Transport in the discrete model as illustrated in Fig. 2a is arranged by the transition probabilities T_{ik} between each pair of sites (i, k) such that the flow of particles or the transition rate from site k to site i is given by $T_{ik}n_k$, where n_k denotes the number of particles or charge carriers at site k. The principle of detailed balance states that in thermal equilibrium the transition rates for each pair of states is balanced, i.e.,

$$T_{ik} n_k^0 = T_{ki} n_i^0 \,, \tag{9}$$

where n_k^0 and n_i^0 denote the respective equilibrium concentrations. Equation (9) suggests that transition rates $T_{ik}n_k$ might be rewritten by $L_{ik}v_k$ where $L_{ik} = T_{ik}n_k^0$ is a normalized rate constant and $v_k = n_k/n_k^0$ is the particle concentration normalized to its equilibrium value. Because of Eq. (9), we have the symmetry

$$L_{ik} = L_{ki} \,, \tag{10}$$

for the reduced matrix L_{ik}. Note that this symmetry is *equivalent* to the validity of detailed balance.

Let us now consider the total balance of carriers at site i that must be zero for any steady state solution. We write

$$\sum_k L_{ik} v_k + g_i^{\mathrm{eq}} + g_i^{\mathrm{exc}} = 0 \,, \tag{11}$$

where the non-diagonal elements of L_{ik} are the normalized transfer rates and the diagonal elements are defined by

$$L_{ii} = -\sum_{i \neq k} L_{ki} - \frac{n_i^0}{\tau_i} . \tag{12}$$

The diagonal elements account the losses at site i due to transitions to the other sites or to any kind of recombination quantified by the lifetime τ_i. The system of Eq. (11) is connected to a heat bath, e.g., the phonon system of a semiconductor and/or the radiation field outside of the system. This connection is represented by the equilibrium generation rate g_i^{eq} for each site i. In addition there shall be an excess generation rate g_i^{exc} that is provided by an extra irradiation of the solar cell by sunlight and by the electrical contacts to the solar cell. In thermal equilibrium we have $g_i^{\mathrm{exc}} = 0$ and $\nu_k = 1$ for all sites i, k and hence

$$\frac{\mathrm{d}}{\mathrm{d}t} n_i = 0 = \sum_k L_{ik} + g_i^{\mathrm{eq}} = -\frac{n_i^0}{\tau_i} + g_i^{\mathrm{eq}} . \tag{13}$$

The second equality results from Eq. (12) and describes the detailed balance between generation and recombination in thermal equilibrium. Equations (11)–(13) suggest to split the matrix L_{ik} into two parts $L_{ik} = \tilde{L}_{ik} - (n_i^0/\tau_i)\,\delta_{ik}$ where the matrix $\tilde{L}_{ik}$ with the property

$$\sum_k \tilde{L}_{ik} = \sum_i \tilde{L}_{ik} = 0 , \tag{14}$$

describes transport with conservation of particles and the diagonal terms $-(n_i^0/\tau_i)\,\delta_{ik} = -g_i^{\mathrm{eq}}\delta_{ik}$ describe losses that in thermal equilibrium are the detailed balance complement to the equilibrium generation rate g_i^{eq}.

Turning now to the non-equilibrium situation it is convenient to replace the normalized concentration ν_k by the normalized excess concentration $\Delta\nu_k = \nu_k - 1$. Equation (11) then reads

$$\sum_k L_{ik}\,\Delta\nu_k = -g_i^{\mathrm{exc}} . \tag{15}$$

The variables $\Delta\nu_k$ and the external driving force g_i^{exc} might be looked at as vectors and L is then a symmetric operator on this vector space X and it holds for any two elements $\Delta\nu^{(a)}, \Delta\nu^{(b)} \in X$

$$\begin{aligned} &\langle L\,\Delta\nu^{(a)} | \Delta\nu^{(b)} \rangle - \langle \Delta\nu^{(a)} | L\,\Delta\nu^{(b)} \rangle \\ &= \sum_i \sum_k L_{ik}\,\Delta\nu_k^{(a)}\,\Delta\nu_i^{(b)} - \sum_i \sum_k L_{ik}\,\Delta\nu_k^{(b)}\,\Delta\nu_i^{(a)} = 0 , \end{aligned} \tag{16}$$

where $\langle \cdot | \cdot \rangle$ is the vector product in X. Equation (16) is equivalent to Eq. (10) and hence also equivalent to the principle of detailed balance.

Consider now two specific solutions $\Delta\nu^{(a)}$ and $\Delta\nu^{(b)}$ of Eq. (15), resulting from unit excess generation δ_a, δ_b at single sites a and b, respectively. Hence we have $L\,\Delta\nu^{(a)} = -\delta_a$ and $L\,\Delta\nu^{(b)} = -\delta_b$

$$\begin{aligned} \sum_i \sum_k L_{ik}\,\Delta\nu_k^{(a)}\,\Delta\nu_i^{(b)} &= \sum_i \sum_k L_{ik}\,\Delta\nu_k^{(b)}\,\Delta\nu_i^{(a)} \\ = -\sum_i \sum_k \delta_a\,\Delta\nu_i^{(b)} &= -\sum_i \sum_k \delta_b\,\Delta\nu_i^{(a)} \end{aligned} \tag{17}$$

and consequently

$$\Delta\nu_a^{(b)} = \Delta\nu_b^{(a)} . \tag{18}$$

Equation (18) states that excess generation at an arbitrary site a leads to the same (normalized) excess carrier density at site b as excess generation at site b leads to excess carriers at site a.

3.2 Continuous solar cell model In the continuous situation the base of calculations becomes a vector space Y of functions in a finite volume V. The symmetry of an operator $\boldsymbol{L}$ in Y is defined by the analogon of Eq. (16), namely the integral

$$\int_V \{\boldsymbol{L}\,\Delta\nu_1\,\Delta\nu_2 - \boldsymbol{L}\,\Delta\nu_2\,\Delta\nu_1)\}\,\mathrm{d}\boldsymbol{r} = 0 , \tag{19}$$

over the volume V. Equation (19) must be valid for all functions $\Delta\nu_1, \Delta\nu_2 \in Y$ regardless, whether or not we are dealing with functions that represent normalized carrier densities $\nu(\boldsymbol{r}) = n(\boldsymbol{r})/n_0(\boldsymbol{r})$ or normalized *excess* carrier densities $\Delta\nu(\boldsymbol{r}) = [n(\boldsymbol{r}) - n_0(\boldsymbol{r})]/n_0(\boldsymbol{r})$. To prove the equivalence of the principle of detailed balance with Eq. (19) we refer to functions $\nu(\boldsymbol{r}) = n(\boldsymbol{r})/n_0(\boldsymbol{r})$. In this situation, the equivalent of Eq. (11) reads

$$\boldsymbol{L}\nu(\boldsymbol{r}) = -g_{\mathrm{eq}}(\boldsymbol{r}) - g_{\mathrm{exc}}(\boldsymbol{r}) . \tag{20}$$

To evaluate the equilibrium transition rates from a sub-volume A to a sub-volume B and vice versa as shown in Fig. 2b, we consider two solutions $\Delta\nu_a$, $\Delta\nu_b$ of Eq. (20) that fulfill

$$\boldsymbol{L}\,\Delta\nu_A = g_A - a_{AB} , \tag{21}$$

$$\boldsymbol{L}\,\Delta\nu_B = g_B - a_{BA} , \tag{22}$$

where $g_{A/B} = 0$ for $\boldsymbol{r} \notin A/B$ and $a_{AB/BA} = 0$ for $\boldsymbol{r} \notin B/A$, i.e., the generation rates $g_{A/B}$ are non-zero only inside the domains A/B. This implies that we have also switched-off the equilibrium generation rate outside the respective domain. Instead, the generation rates $g_{A/B}$ are chosen such that we have an equilibrium carrier concentration, i.e., $\nu_{A/B} = 1$ inside the domains A/B for every $\boldsymbol{r} \in A/B$. In turn, we have the negative generation (annihilation) rates $a_{AB/BA}$ that are non-zero only in the complementary domain B/A and chosen such that the carrier concentrations vanish in these

domains. Thus, $v_{A/B} = 0$ for every $\boldsymbol{r} \in B/A$. Application of Eq. (20) yields

$$0 = \int_V \{\boldsymbol{L} v_A v_B - \boldsymbol{L} v_B v_A)\}\, \mathrm{d}\boldsymbol{r} = -\int_V \{(g_A - a_{AB})\, v_B - (g_B - a_{BA})\, v_A)\}\, \mathrm{d}\boldsymbol{r}. \quad (23)$$

Because of the restrictions on $g_{A/B}$ on the domains A/B and those of $a_{AB/BA}$ to the domains B/A, we can restrict the integration on the two domains to obtain

$$0 = -\int_A \{g_A v_B - a_{BA} v_A\}\, \mathrm{d}\boldsymbol{r} + \int_B \{g_B v_A - a_{AB} v_A\}\, \mathrm{d}\boldsymbol{r} = \int_A a_{BA}\, \mathrm{d}\boldsymbol{r} - \int_B a_{AB}\, \mathrm{d}\boldsymbol{r}\,, \quad (24)$$

where for the last steps we have used the constrains on $v_{A/B}$ inside the domains A/B. Since for the solution v_A particles are only generated in domain A, the integral

$$A_{AB} = \int_B a_{AB}\, \mathrm{d}\boldsymbol{r}\,, \quad (25)$$

corresponds to the flow of particles into domain B that can only originate from domain A (cf. Fig. 2b). Because of Eq. (24), we have the symmetry $A_{AB} = A_{BA}$, i.e., the principle of detailed balance.

3.3 Making contact To connect the discrete system to the outside world by electrical contacts, we have to modify Eq. (11) according to

$$\sum_k L_{ik} v_k = \sum_k (\tilde{L}_{ik} - g_i^{\mathrm{eq}} \delta_{ik} - S_i \delta_{ik})\, v_k = -g_i^{\mathrm{eq}} - g_i^{\mathrm{exc}} - S_i \left[\exp\left(\frac{qV_j}{kT}\right)\right], \quad (26)$$

where V_j is the voltage that drops at the rectifying and collecting junction and kT/q is the thermal voltage. Note that we only discuss injection and extraction of minority carriers, while the particle of the other polarity is assumed to be perfectly connected to the second contact shown in Fig. 2. In addition, we assume that the minority carrier contact behaves according to the ideal diode law, implying that the following investigation is only valid as long as the junction is well approximated by the ideal diode law. In Chapter 7, we will discuss deviations from the ideal diode law, i.e. situations where the contact is defined differently like in a pin-junction diode.

The term $S_j \delta_{jk} v_k$ adds to the diagonal elements of the matrix L_{ik} describing the extraction of carriers via the junction. Note that we have $S_i > 0$ for all sites that are connected to a junction (i.e., $i = j$ in Fig. 2a) and $S_i = 0$ for non-junction sites. Obviously, the thermal equilibrium solution $v_k = 1$ fulfills Eq. (26) for $V_i = 0$ and $g_i^{\mathrm{exc}} = 0$. We may rewrite Eq. (26) in terms of the normalized excess carrier density Δv by

$$\sum_k L_{ik}\, \Delta v_k = \sum_k (\tilde{L}_{ik} - g_i^{\mathrm{eq}} \delta_{ik} - S_i \delta_{ik})\, \Delta v_k = -g_i^{\mathrm{exc}} - S_i \left[\exp\left(\frac{qV_i}{kT}\right) - 1\right]. \quad (27)$$

We emphasize here that from Eq. (27) it is straightforward to derive Donolato's reciprocity relation [27] that connects the collection efficiency of minority carriers to the dark carrier distribution. This has been shown in Ref. [26] for a somewhat different definition of the contacts. Donolato's relation has been used as an intermediate step to derive the opto-electronic reciprocity between electroluminescent emission and photovoltaic quantum efficiency [28]. In the following we use a more direct way for proving this theorem by considering the incoming and outgoing light rays explicitly.

3.4 Opto-electronic reciprocity For the last step we have to introduce light absorption by generation of an electron/hole pair into our system. This process is complemented by radiative recombination of said pair in order to comply with the principle of detailed balance. For the light emitted by radiative recombination at a site i we define the radiative lifetime τ_i^{rad} by the equilibrium equation

$$\frac{n_i^0}{\tau_i^{\mathrm{rad}}} = \frac{n_i^0}{\tau_i^{\mathrm{rad}}} \left[\sum_{k \neq i} P_{ik} + \sum_l E_{il} + \sum_{l'} E_{il'}\right] = \sum_{k \neq i} P_{ki} \frac{n_k^0}{\tau_k^{\mathrm{rad}}} + \sum_l F_{il} \phi_l^{\mathrm{bb}} + \sum_{l'} F_{il'} \phi_{l'}^{\mathrm{bb}} = g_i^{\mathrm{eq}}\,, \quad (28)$$

where radiative recombination is counterbalanced by the equilibrium generation rate g_i^{eq}. Both, the recombination and the generation term in Eq. (28) are split in three parts according to the consequences of the photon emission: (1) the light is reabsorbed by generation of another electron/hole pair somewhere else (say at site k) in the sample (photon recycling), (2) the light is emitted from the surface of the sample in a direction and wavelength interval l (cf. Fig. 2a), or (3) the light is parasitically absorbed if it leaves the sample in a direction and wavelength interval l'. Note that the indices l and l' simultaneously run over two physical quantities, namely over the direction and over the wavelength intervals of the incoming and outgoing light.

The first case (1) introduces a non-local interaction into our system where a charge carrier vanishes at site i and re-appears at site k with a probability P_{ik}. In thermal equilibrium this process is quantitatively counterbalanced by radiative recombination at site k with generation of a carrier at site i. Therefore, we define the (off-diagonal) matrix elements

$$L_{ik}^{\mathrm{PR}} = P_{ik} \frac{n_i^0}{\tau_i^{\mathrm{rad}}} = P_{ki} \frac{n_k^0}{\tau_k^{\mathrm{rad}}} = L_{ki}^{\mathrm{PR}}\,, \quad (29)$$

where the symmetry $L_{ik}^{\mathrm{PR}} = L_{ki}^{\mathrm{PR}}$ results again from the principle of detailed balance. The diagonal elements are given by

$$L_{ii}^{\mathrm{PR}} = -\sum_{i \neq k} L_{ik}^{\mathrm{PR}} \,. \tag{30}$$

In non-equilibrium, the net balance of carriers at site i by (recycled) radiative recombination is given by

$$\begin{aligned}\left(\frac{\mathrm{d}}{\mathrm{d}t} n_i\right)_{PR} &= -\nu_i \sum_{k \neq i} L_{ik}^{\mathrm{PR}} + \sum_{k \neq i} L_{ki}^{\mathrm{PR}} \nu_k \\ &= \sum_k L_{ki}^{\mathrm{PR}} \nu_k = \sum_k L_{ki}^{\mathrm{PR}} \, \Delta\nu_k \,. \end{aligned} \tag{31}$$

Obviously steady state is achieved in equilibrium ($n_k = 1$, $\Delta n_k = 0$) and for any constant reduced (excess) carrier concentration. Further, Eq. (30) warrants that no carrier is lost in the system in any non-equilibrium situation. Thus we can implement the photon recycling matrix L_{ik}^{PR} into the carrier conserving part $\tilde{L}_{ik}$ of the reduced transport matrix of Eqs. (12) and (27).

For case (2) the emission of a photon from site i into a direction and wavelength interval l (with the emission probability E_{il}) must be counterbalanced in thermal equilibrium by the (black body) equilibrium irradiation *from* direction and wavelength interval l that generates a charge carrier at i with F_{li} as the rate constant. Consequently, we have

$$G_{il} = E_{il} \frac{n_i^0}{\tau_i^{\mathrm{rad}}} = F_{li} \phi_l^{\mathrm{bb}} = G_{li} \,. \tag{32}$$

The balance equation resulting from photon emission and absorption then reads

$$\begin{aligned}\left(\frac{\mathrm{d}}{\mathrm{d}t} n_i\right)_{\mathrm{em/abs}} &= -\nu_i \sum_l G_{il} + \sum_l G_{il} \varphi_l \\ &= -\Delta\nu_i \sum_l G_{il} + \sum_l G_{il} \, \Delta\varphi_l \,, \end{aligned} \tag{33}$$

where $\varphi_l = \phi_l / \phi_l^{\mathrm{bb}}$ and $\Delta\varphi_l = \varphi_l - 1$ are normalized photon fluxes and excess photon fluxes, respectively.

For case (3), i.e. photon emission into direction and wavelength intervals l' with parasitic absorption, an equation analogous to Eq. (32) is valid. However, the solar cell obtains no excess radiation from those directions. Therefore, the balance equation reads

$$\left(\frac{\mathrm{d}}{\mathrm{d}t} n_i\right)_{\mathrm{par}} = -\nu_i \sum_{l'} G_{il'} + \sum_{l'} G_{il'} = -\Delta\nu_i \sum_{l'} G_{il'} \,. \tag{34}$$

Note that radiative recombination with subsequent parasitic absorption is a real loss term. I.e. the recombined carrier does not re-appear at another site like in the photon recycling balance, Eq. (31), nor does it show up as a photon leaving the device as in the balance of emission/absorption, Eq. (33). Therefore, we may include this term into a general non-radiative loss term

$$\left(\frac{\mathrm{d}}{\mathrm{d}t} n_i\right)_{\mathrm{nr}} = -\frac{n_i^0}{\tau_i^{\mathrm{nr}}} \Delta\nu_i \,, \tag{35}$$

with a general non-radiative recombination lifetime τ_i^{nr}.

By setting the balance Eqs. (31), (33) and (35) for the radiative and non-radiative mechanisms into Eq. (27) we obtain

$$\begin{aligned}\sum_k L_{ik} \, \Delta\nu_k &= \sum_k \tilde{L}_{ik} \, \Delta\nu_k - \left(\frac{n_i^0}{\tau_i^{\mathrm{nr}}} + S_i + \sum_{l'} G_{il'}\right) \Delta\nu_i \\ &= -\sum_l G_{il} \, \Delta\varphi_l - S_i \left[\exp\left(\frac{qV_j}{kT}\right) - 1\right]. \end{aligned} \tag{36}$$

Equation (36) contains the particle conserving matrix $\tilde{L}_{ik}$ that contains now also all photon recycling terms. In addition, we have the loss term due to all types of non-radiative recombination including parasitic absorption. The extraction term of excess carriers to the junction in the middle part is complemented by an analogous injection term in the lower line. Likewise, the radiative recombination term due to emission of photons in all directions and wavelength intervals l is complemented by a photogeneration term caused by excess photons impinging from all those directions.

We now apply Eq. (16) to two specific solutions of Eq. (36): the solution $\Delta\nu^{(\mathrm{sc})}$ for the short circuit situation under illumination (from a single direction and in a certain wavelength interval l) fulfilling

$$\sum_k L_{ik} \, \Delta\nu_k^{(\mathrm{sc})} = -G_{il} \, \Delta\varphi_l \tag{37}$$

and a solution $\Delta\nu^{(\mathrm{dark})}$ for the dark situation with voltage V applied to the junction connected to site i

$$\sum_k L_{ik} \, \Delta\nu_k^{(\mathrm{dark})} = -S_i \left[\exp\left(\frac{qV}{kT}\right) - 1\right]. \tag{38}$$

Using Eqs. (37) and (38) to replace the two sums over k from Eq. (16), we obtain

$$\begin{aligned}&\langle L \, \Delta\nu^{(\mathrm{sc})} | \, \Delta\nu^{(\mathrm{dark})} \rangle - \langle \Delta\nu^{(\mathrm{sc})} | \, L \, \Delta\nu^{(\mathrm{dark})} \rangle \\ &= -\sum_i G_{il} \, \Delta\varphi_l \, \Delta\nu_i^{(\mathrm{dark})} + S_i \, \Delta\nu_i^{(\mathrm{sc})} \left[\exp\left(\frac{qV}{kT}\right) - 1\right] = 0 \,. \end{aligned} \tag{39}$$

Note that the quantity $\Delta\varphi_l$ in Eq. (39) is the *incident* normalized excess photon flux whereas the photon flux *emitted* into direction/wavelength l is given by

$$\Delta\varphi_l^{\mathrm{em}} = -\sum_i G_{il} \, \Delta\nu_i^{(\mathrm{dark})} \,. \tag{40}$$

For the illuminated case, the short circuit current collected by the junction (interpreted in terms of collected particles by unit time) reads $j_{\mathrm{sc}}^{(l)} = S_i \nu_i^{(\mathrm{sc})}$. For the specific direction

and wavelength of the excess illumination $\Delta\varphi_l$ we define therefore the external quantum efficiency via

$$Q_{\mathrm{e}}^{(l)} = \frac{S_i v_i^{(\mathrm{sc})}}{\Delta\varphi_l} = \frac{j_{\mathrm{sc}}^{(l)}}{\Delta\varphi_l} . \tag{41}$$

Setting Eqs. (40) and (41) into (39) finally yields

$$\Delta\varphi_l = Q_{\mathrm{e}}^{(l)} \left[\exp\left(\frac{qV}{kT}\right) - 1 \right], \tag{42}$$

which is a reciprocity relation between electroluminescent emission and solar cell quantum efficiency [28] that holds for photons of any energy entering the solar cell under any angle and at any surface position.

By removing the normalization from Eq. (42) and by referring to the routinely measured external quantum efficiency $Q_{\mathrm{e}}(\lambda)$ under normal incidence as a function of the wavelength λ, the reciprocity relation describes the spectral electroluminescent emission of the device

$$\Delta\phi_{\mathrm{em}}(\lambda) = Q_{\mathrm{e}}(\lambda)\, \phi_{\mathrm{bb}}(\lambda) \left[\exp\left(\frac{qV}{kT}\right) - 1 \right] \tag{43}$$

in a more common form.

3.5 Continuous case The derivation of Eq. (42) in the continuous case follows analogously. We define a function G which depends on the light path and thus on the surface position A_{S} and the solid angle Ω under which the photon enters or leaves the cell as well as on the photon energy E. We replace the sum in the discrete case by integrals over A_{S} and Ω and arrive at

$$\begin{aligned} \boldsymbol{L}\,\Delta\nu &= \left(\tilde{\boldsymbol{L}} - \frac{n_0(\boldsymbol{r})}{\tau(\boldsymbol{r})} - S(\boldsymbol{r})\,\delta_j(x) \right) \Delta\nu(\boldsymbol{r}) \\ &\quad - \int_{A_{\mathrm{S}}} \int_{\Omega} \int_0^{\infty} G(\boldsymbol{r}, A_{\mathrm{S}}, \Omega, E)\, \Delta\nu(\boldsymbol{r})\, \mathrm{d}\Omega\, \mathrm{d}A_{\mathrm{S}}\, \mathrm{d}E \\ &= - \int_{A_{\mathrm{S}}} \int_{\Omega} \int_0^{\infty} G(\boldsymbol{r}, A_{\mathrm{S}}, \Omega, E)\, \Delta\varphi(A_{\mathrm{S}}, \Omega, E)\, \mathrm{d}\Omega\, \mathrm{d}A_{\mathrm{S}}\, \mathrm{d}E \\ &\quad - S(\boldsymbol{r})\,\delta_j(\boldsymbol{r}) \left[\exp\left(\frac{qV_j}{kT}\right) - 1 \right]. \end{aligned} \tag{44}$$

Note that for the definition of the contact we make use of a two-dimensional delta-distribution δ_j, that allows us to integrate over all coordinates $\boldsymbol{r}_j$ at those surfaces A_j of the device that are connected to the junction (cf. Fig. 2b). We define this delta distribution δ_j such that it fulfills

$$\int_V \delta(\boldsymbol{r} - \boldsymbol{r}_j)\, f(\boldsymbol{r})\, \mathrm{d}\boldsymbol{r} = \int_{A_j} f(\boldsymbol{r}_j)\, \mathrm{d}A_j , \tag{45}$$

for all functions $f \in Y$. We use this definition of a junction for two reasons:

First, the symmetry property of the operator $\boldsymbol{L}$ depends on the boundary conditions. The above definition of the junction leaves the boundary conditions for $\boldsymbol{L}$ and thus its symmetry untouched. We therefore avoid the somewhat cumbersome discussion of different boundary conditions in different bias situations (see e.g. Ref. [29]). However in the limit $S(\boldsymbol{r}_j) \to \infty$, the usual situation is recovered.

Second, the feature of a finite collection velocity $S(\boldsymbol{r}_j)$ at the junction is physically important in situations where the concentration $\Delta\nu$ does not represent the normalized excess minority carrier concentration but refers to the exciton density in excitonic solar cells where $S(\boldsymbol{r}_j)$ obtains the meaning of a dissociation velocity of excitons into electrons and holes [30].

Note that in all respects Eq. (44) is the continuous equivalent to Eq. (36). Especially the operator $\tilde{\boldsymbol{L}}$ contains a photon recycling part $\boldsymbol{L}_{\mathrm{PR}}$ that is defined by the integral kernel

$$\boldsymbol{L}_{\mathrm{PR}}\,\nu(\boldsymbol{r}) = \int_V \kappa(\boldsymbol{r}, \boldsymbol{r}')\, \nu(\boldsymbol{r}')\, \mathrm{d}\boldsymbol{r}' . \tag{46}$$

Because of the symmetry $\kappa(\boldsymbol{r}, \boldsymbol{r}') = \kappa(\boldsymbol{r}', \boldsymbol{r})$, $\boldsymbol{L}_{\mathrm{PR}}$ is also a symmetric operator [28, 31].

All non-radiative terms in Eq. (44) are contained in the factor n_0/τ which is a simple multiplicator and, consequently, also symmetric. The interaction with the external radiation field by emission and absorption is represented on the right as well as on the left of Eq. (44) by the triple integrals over the angles and the energy of the emitted light as well as over the surface A_{S} of the sample. The reciprocity of light emission and absorption is reflected in the fact that the *same* function $G(\boldsymbol{r}, A_{\mathrm{S}}, \Omega, E)$ is used on the right of Eq. (44) for *light emission* as well as on the left for *light absorption*. This fact corresponds to the symmetry of G_{il} for the discrete case as given in Eq. (32).

Now, we make use of the symmetry of the operator $\boldsymbol{L}$ and apply Eq. (19) on the same two situations as in the discrete case. The short circuit situation (with $V_j = 0$) responds to an excitation by light from a certain direction Ω' at a given photon energy E' that enters only at a given location $\boldsymbol{r}_{\mathrm{s}}$ out of the area A_{s}. Thus, we write this excess photon flux as

$$\Delta\varphi\,(\Omega, A_{\mathrm{S}}, E) = \Delta\varphi\delta\,(\Omega')\,\delta(\boldsymbol{r}_{\mathrm{S}})\,\delta(E') . \tag{47}$$

Since the excess photon flux $\Delta\varphi$ is made up of three delta distributions, the integrals from Eq. (44) vanish for the solution under illumination leading to

$$\begin{aligned} \boldsymbol{L}\,\Delta\nu^{(\mathrm{sc})} &= - \int_{A_{\mathrm{S}}} \int_{\Omega} \int_0^{\infty} G(\boldsymbol{r}, A_{\mathrm{S}}, \Omega, E)\, \Delta\varphi\,(A_{\mathrm{S}}, \Omega, E)\, \mathrm{d}\Omega\, \mathrm{d}A_{\mathrm{S}}\, \mathrm{d}E \\ &= G(\boldsymbol{r}, \boldsymbol{r}_{\mathrm{S}}, \Omega', E')\, \Delta\varphi . \end{aligned} \tag{48}$$

The solution $\Delta\nu^{(\mathrm{dark})}$ for the dark situation (note: $G = 0$) with voltage V_j applied to the junction connected to site i follows directly from Eq. (44) as

$$\boldsymbol{L}\,\Delta\nu^{(\mathrm{dark})} = - S(\boldsymbol{r})\,\delta_j(\boldsymbol{r}) \left[\exp\left(\frac{qV_j}{kT}\right) - 1 \right]. \tag{49}$$

To connect the situation under illumination and short circuit with the situation in the dark under applied voltage, we reformulate Eq. (19) for the current situation. Because of the symmetry of $\boldsymbol{L}$, we have

$$\int_V \left\{ \boldsymbol{L}\, \Delta\nu^{(\mathrm{sc})}\, \Delta\nu^{(\mathrm{dark})} - \boldsymbol{L}\, \Delta\nu^{(\mathrm{dark})}\, \Delta\nu^{(\mathrm{sc})} \right\} \mathrm{d}\boldsymbol{r} = 0\,. \tag{50}$$

If we now insert Eqs. (48) and (49) into the symmetry relation, we receive a connection between $\Delta\nu^{(\mathrm{dark})}$ and $\Delta\nu^{(\mathrm{sc})}$, namely

$$\int_V G(\boldsymbol{r}, \boldsymbol{r}_\mathrm{S}, \Omega', E')\, \Delta\varphi\, \Delta\nu^{(\mathrm{dark})}(\boldsymbol{r})\, \mathrm{d}\boldsymbol{r}$$

$$= \int_V S(\boldsymbol{r})\, \delta_j(\boldsymbol{r} - \boldsymbol{r}_j)\, \Delta\nu^{(\mathrm{sc})}(\boldsymbol{r})\, \mathrm{d}\boldsymbol{r} \left[\exp\left(\frac{qV_j}{kT} \right) - 1 \right]. \tag{51}$$

Since $\Delta\varphi$ is a mere number independent from the coordinate $\boldsymbol{r}$, we may excerpt this term from the integral. The remaining integral the corresponds to the electroluminescent emission due to the injected excess dark carrier concentration $\Delta\nu^{(\mathrm{dark})}$, i.e.

$$\Delta\varphi_{\mathrm{em}}(\boldsymbol{r}_\mathrm{S}, \Omega', E') = \int_V G(\boldsymbol{r}, \boldsymbol{r}_\mathrm{S}, \Omega', E')\, \Delta\nu^{(\mathrm{dark})}(\boldsymbol{r})\, \mathrm{d}\boldsymbol{r}\,. \tag{52}$$

On the right hand side of Eq. (51), we may identify the integral term by the short circuit current density caused by the excess carrier concentration $\Delta\nu^{(\mathrm{sc})}$ due to illumination. We thus have

$$j_{\mathrm{sc}}(\boldsymbol{r}_\mathrm{S}, \Omega', E') = \int_V S(\boldsymbol{r})\, \delta_j(\boldsymbol{r} - \boldsymbol{r}_j)\, \Delta\nu^{(\mathrm{sc})}(\boldsymbol{r})\, \mathrm{d}\boldsymbol{r}\,, \tag{53}$$

where j_{sc}, understood as a particle current, depends on the energy E' and on the direction Ω' of the photons that enter the solar cell at the surface coordinate $\boldsymbol{r}_\mathrm{S}$ in order to create the specific carrier concentration $\Delta\nu^{(\mathrm{sc})}$ that we consider at the moment. With Eqs. (52)–(53) reduces to

$$\Delta\varphi_{\mathrm{em}}(\boldsymbol{r}_S, \Omega', E')\, \Delta\varphi = j_{\mathrm{sc}}(\boldsymbol{r}_\mathrm{S}, \Omega', E') \left[\exp\left(\frac{qV_j}{kT} \right) - 1 \right]. \tag{54}$$

Reorganization of Eq. (54) leads to

$$\Delta\varphi_{\mathrm{em}}(\boldsymbol{r}_\mathrm{S}, \Omega', E') = \frac{j_{\mathrm{sc}}(\boldsymbol{r}_\mathrm{S}, \Omega', E')}{\Delta\varphi} \left[\exp\left(\frac{qV_j}{kT} \right) - 1 \right]$$

$$= Q_{\mathrm{e}}(\boldsymbol{r}_\mathrm{S}, \Omega', E') \left[\exp\left(\frac{qV_j}{kT} \right) - 1 \right], \tag{55}$$

i.e., the reciprocity relation connecting the electroluminescent emission $\Delta\varphi_{\mathrm{em}}(\boldsymbol{r}_\mathrm{S}, \Omega', E')$ at photon energy E' into the direction Ω' leaving the cell at the surface coordinate $\boldsymbol{r}_\mathrm{S}$ with the external quantum efficiency $Q_{\mathrm{e}}(\boldsymbol{r}_\mathrm{S}, \Omega', E')$ for light with the same photon energy entering the cell at the same spot from the same angle. Thus, the opto-electronic reciprocity [28] as expressed by Eq. (43) for the discrete case is here proven for the continuous case with largely analogical arguments.

4 Two simple examples The derivation presented above follows the most direct way to connect the short circuit current to the luminescence. However, this opto-electronic reciprocity is only one of several important symmetry and reciprocity relations that connect different situations in the same device with each other. Thus, we want to discuss two other relations by introducing two simple examples, one for a discrete and one for a continuos solar cell.

4.1 A two state solar cell model In order to study the implications of the above derivations, we want to reduce the solar cell to its crucial components. For a discrete solar cell, there are exactly two distinct states fundamentally necessary. One state that absorbs photons and creates electron/hole pairs and one state that collects the minority carrier, for instance the electron (Fig. 3).

We define one constant a for the radiative coupling between photons and electron/hole pair. In the same way, we define the constant b for non-radiative coupling and the constant c for the coupling of the absorber state with the normalized electron concentration in the contact ω. Due to the principle of detailed balance [see Eq. (10)], the differential equation for the normalized concentration ν of electrons in the absorber state is

$$\frac{\partial \nu}{\partial t} = -a\nu + a\varphi - b\nu + b - c\nu + c\omega\,. \tag{56}$$

The boundary condition for the concentration of electrons in the contact is given by the ideal diode law

$$\omega = \exp\left(qV/kT\right). \tag{57}$$

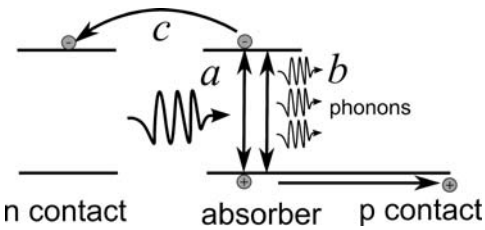

Figure 3 Scheme of a discrete solar cell model with the smallest possible number of states, namely two – one for the minority carrier contact and one for the absorber. The system is defined by the transition rates a for radiative coupling of photons and electron/hole pairs, b for the non-radiative coupling of electron/hole pairs with the phonon bath and c the coupling between the absorber and the contact. We assume that the majorities are extracted with unity efficiency and thus do not have to consider the hole contact as a separate state.

In the steady state situation $\partial \nu/\partial t = 0$, we find for the concentration ν

$$\nu = \frac{a\varphi + b + c\exp(qV/kT)}{a+b+c} \tag{58}$$

and for the normalized excess carrier concentration $\Delta\nu = \nu - 1$

$$\Delta\nu = \frac{a\,\Delta\varphi + c[\exp(qV/kT) - 1]}{a+b+c}, \tag{59}$$

where $\Delta\varphi = \varphi - 1$ is the normalized excess photon flux. As for the derivation of the Shockley–Queisser limit, we investigate now both the photocurrent and the recombination current.

The recombination current follows from the concentration of minorities in the dark, i.e. for $\Delta\varphi = 0$. The normalized excess dark carrier concentration is then

$$\Delta\nu_{\mathrm{dark}} = \frac{c}{a+b+c}[\exp(qV/kT) - 1]. \tag{60}$$

The concentration under illumination is

$$\Delta\nu_{\mathrm{illu}} = \frac{a\,\Delta\varphi}{a+b+c} \tag{61}$$

and the collection efficiency f_{c} of electrons, which determines the photocurrent, is

$$f_{\mathrm{c}} = \frac{c\,\Delta\nu_{\mathrm{illu}}}{a\,\Delta\varphi} = \frac{c}{a+b+c}. \tag{62}$$

We note that the collection efficiency f_{c}, defined as the flux of electrons flowing from our single absorber state to the contact, normalized to the excess flux of photons being absorbed, equals the normalized dark carrier concentration $\Delta\nu_{\mathrm{dark}}/(\omega - 1)$. This relation, connecting the injection of carriers in the dark to the extraction of carriers under illumination is known as the reciprocity theorem of Donolato [27]. Just like the SQ-limit, the Donolato theorem is a direct consequence of the principle of detailed balance [26]. It holds not only in the simplified world of our two state solar cell model but also for continuous systems, with spatial variation of all given parameters [29, 32, 33].

Having discussed the relation between photo- and recombination current, we go one step further and discuss the case of light absorption and photocurrent generation in our discrete solar cell with the inverse case of carrier injection and light emission.

Let us assume that our single absorbing state has a certain distance to the device surface. Optically relevant is the transmittance T that depends on this distance and is defined by the requirement that the absorbed photon flux $a\varphi$ depends on the photon flux φ_{surf} impinging on the solar cell surface via

$$a\varphi = Ta\varphi_{\mathrm{surf}}. \tag{63}$$

Now, we define a quantum efficiency Q as the number of collected minorities (electrons) per photon impinging on the surface of our device as

$$Q = \frac{c\nu}{\varphi_{\mathrm{surf}}} = \frac{c\nu}{a\varphi}\frac{a\varphi}{\varphi_{\mathrm{surf}}} = f_{\mathrm{c}}aT. \tag{64}$$

Turning now to the light emitting diode situation, we have to calculate the photon flux emitted from the surface of the device caused by radiative recombination in our single absorber state. The amount of light created by recombination follows from the rate Eq. (56) as $a\nu$. The amount of light that is emitted by the surface is damped by the factor T accounting now for reabsorption of emitted photons. Thus, the emission follows as

$$\varphi_{\mathrm{em}} = a\nu T = aT\frac{c}{a+b+c}\exp(qV/kT). \tag{65}$$

Using $f_{\mathrm{c}} = c/(a + b + c)$ and Eq. (47), we find that the emission relates to the quantum efficiency as

$$\varphi_{\mathrm{em}} = Q\exp(qV/kT). \tag{66}$$

Thus, we derived directly from the principle of detailed balance two reciprocity relations, one between the photocarrier collection and carrier injection and one between the solar cell quantum efficiency and the electroluminescence (EL).

4.2 The one sided pn-junction device Up to now, we gave a very general proof for the reciprocity relations and subsequently discussed them in a rather abstract environment consisting only of two discrete states. Thus, we consider it important to have a final look on a model of a solar cell, which is probably more familiar to the reader. We choose the case of an abrupt one sided pn-junction, which is a decent approximation of e.g. crystalline silicon solar cells, where the whole device consists mostly of one p-type layer, with only a thin n^{+}-emitter on top. This approximation has the advantage that we again only have to consider minorities – in this case electrons. In contrast to the three dimensional derivation discussed in Section 3, we now consider only one coordinate x parallel to the surface normal of the solar cell and neglect all lateral variations.

The detailed balance between radiative recombination and photogeneration in terms of commonly used quantities like lifetime τ and absorption α coefficient is given by [34]

$$\frac{n_0}{\tau} = \alpha\phi_{\mathrm{bb}}, \tag{67}$$

where n_0 is the equilibrium concentration of minorities. The (energy resolved) radiative recombination rate r_{rad} at position x follows directly from the previous Eq. (67) if we allow for excess minority carriers Δn as

$$r_{\mathrm{rad}}(x, E) = \frac{\Delta n(x)}{\tau} = \alpha\phi_{\mathrm{bb}}\frac{\Delta n(x)}{n_0}. \tag{68}$$

The electroluminescent emission depends on the rate describing radiative recombination and the probability f_{em} that the created photons are not reabsorbed and follows then from the integral

$$\phi_{em}(x, E) = \int_0^w r_{rad}(x, E)\, f_{em}(x)\, dx\,, \tag{69}$$

over the thickness w of the device. Although we don't know the emission probability f_{em} of photons we can derive it from Würfel's generalized Planck's law (Eq. (2)). We know that for flat quasi-Fermi levels and thus a constant quasi-Fermi level split ΔE_F

$$\phi_{em} = \int_0^w \alpha f_{em}(x)\, dx\, \phi_{bb} \exp\left(\frac{\Delta E_F}{kT}\right) = a(E)\, \phi_{bb} \exp\left(\frac{\Delta E_F}{kT}\right), \tag{70}$$

holds. Since the absorptance

$$a(E) = \int_0^w g(x, E)\, dx\,, \tag{71}$$

is the integral over the generation rate g, we find

$$\alpha f_{em}(x) = g(x) \tag{72}$$

and finally the EL spectrum also for non-flat quasi-Fermi levels

$$\phi_{em} = \int_0^w g(x) \frac{\Delta n(x)}{\Delta n_j}\, dx\, \phi_{bb} \exp\left(\frac{qV}{kT}\right). \tag{73}$$

Note that the voltage V is defined as the splitting of quasi-Fermi levels at the collecting junction for the minority carriers. Thus, the excess carrier concentration Δn_j at the junction is given by

$$\Delta n_j = n_0[\exp(qV/kT) - 1]\,. \tag{74}$$

This Eq. (74) is equivalent to our definition of ω in Eq. (57) for the discrete case. Note that the generation rate $g(x)$ is defined such that it has the unit [cm^{-1}]. It relates to the commonly used generation rate G in [cm^{-3} s^{-1}] as G normalized to the incoming photon flux ϕ_{in}, i.e. $g = G/\phi_{in}$.

In order to show that the emission spectrum defined by Eq. (73) is identical to the result obtained for the discrete model [Eq. (66)], we need to define the quantum efficiency in a similar way as done in Eq. (64). Since the quantum efficiency describes a series connection of photocarrier generation and collection, it is useful to write the quantum efficiency as

$$Q_e(E) = \int_0^w g(x, E)\, f_c(x)\, dx\,, \tag{75}$$

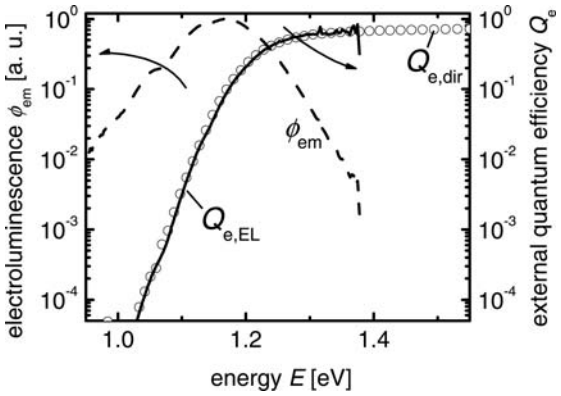

Figure 4 Measurement of an EL spectrum ϕ_{em} of a Cu(In,Ga)Se_2 solar cell, which allows us to compute the solar cell quantum efficiency Q_e by solving Eq. (77) for the quantum efficiency. We then obtain the quantum efficiency $Q_{e,EL}$ derived from the EL measurement in relative units. A direct measurement of the quantum efficiency $Q_{e,dir}$ allows us to scale $Q_{e,EL}$ and to verify that the relative shape of $Q_{e,EL}$ and $Q_{e,dir}$ are equal.

i.e. integral over the product of two quantities: the generation rate g and the collection efficiency f_c. Thus, by application of Donolato's theorem,

$$f_c(x) = \frac{\Delta n_D(x)}{\Delta n_{Dj}} = \frac{\Delta n_D(x)}{n_0(x)[\exp(qV/kT) - 1]}\,, \tag{76}$$

we directly obtain the reciprocity between electroluminescent emission and photovoltaic quantum efficiency for the continuos case [28]

$$\Delta\phi_{em}(E) = Q_e(E)\, \phi_{bb}(E) \left[\exp\left(\frac{qV}{kT}\right) - 1\right]. \tag{77}$$

Figure 4 illustrates the meaning and the experimental verification [35] of Eq. (77). The measurement of an EL spectrum of a Cu(In,Ga)Se_2 solar cell allows us to compute the solar cell quantum efficiency Q_e by solving Eq. (77) for the quantum efficiency. We then obtain the quantum efficiency $Q_{e,EL}$ derived from the EL measurement in relative units. A direct measurement of the quantum efficiency $Q_{e,dir}$ allows us to scale $Q_{e,EL}$ and to verify that the relative shape of $Q_{e,EL}$ and $Q_{e,dir}$ are equal.

5 Solar cell and light emitting diode The fundamentals section started with the SQ-limit, i.e. with the perfect solar cell. The case of perfect absorption above the band gap, infinite carrier mobilities and suppressed non-radiative recombination is also the limiting situation for a light emitting diode (LED). It seems that for less ideal devices, the requirements for LEDs and solar cells differ considerably. Organic LEDs [36] for instance have very high LED quantum efficiencies $Q_{LED} \approx 15\%$ [37], while solar cells made from polymers have just reached only 5% power conversion efficiency [38]. Silicon devices, however, are among the best single junction solar cells, with efficiencies $\eta = 24.7\%$ [39], however light emission from

silicon is rather inefficient with highest LED quantum efficiencies approaching $Q_{LED} = 1\%$ [40]. Thus, although the reciprocity relation [Eq. (77)] suggests a strong link between the light emitting and light absorbing situation, there seems to be no direct relationship between LED quantum efficiency and solar cell efficiency.

However, as shown in Refs. [28, 35, 41, 42], the photovoltaic quantity that actually relates most directly to the LED quantum efficiency is the open circuit voltage V_{oc}. In photovoltaics, a frequently used measure for the amount of recombination is to relate the V_{oc} to the band gap E_g either by taking the ratio qV_{oc}/E_g or the difference $E_g - qV_{oc}$ [43]. If we instead relate the measured V_{oc} to its radiative limit

$$V_{oc}^{rad} = \frac{kT}{q} \ln\left(\frac{J_{sc}}{J_{0,rad}} + 1\right) \approx \frac{kT}{q} \ln\left(\int_0^\infty Q_e \phi_{sun}\, dE \Big/ \int_0^\infty Q_e \phi_{bb}\, dE\right), \tag{78}$$

as defined by detailed balance, we see a direct correlation to the LED quantum efficiency. The difference of limiting and real V_{oc} gives

$$\Delta V_{oc} = V_{oc}^{rad} - V_{oc} = -\frac{kT}{q} \ln\left(Q_{LED}\right), \tag{79}$$

since the LED quantum efficiency Q_{LED} is defined as

$$Q_{LED}(V) = \frac{J_{rad}(V)}{J_{nr}(V) + J_{rad}(V)}. \tag{80}$$

Here, J_{rad} denotes the radiative recombination current and J_{nr} the non-radiative recombination current.

This result shows that LED quantum efficiency and thus the amount of additional non-radiative recombination compared to the radiative one directly correlates with open circuit voltage. This provides us with the reasons for the apparent discrepancy between the requirements for good solar cell and LED materials. A high percentage of radiative recombination is the paramount requirement for efficient LEDs, while indirect semiconductors with their very long radiative lifetimes are not well suited for application in light emitting devices. Of course, they also suffer from their long radiative lifetimes compared to the non-radiative ones in terms of their V_{oc}. However, these losses only enter the V_{oc} and thus the efficiency logarithmically. For instance, a difference of radiative and non-radiative V_{oc} of only 60 meV corresponds to a dramatic difference in Q_{LED} of one order of magnitude. The reason, why organic polymers have difficulties in becoming high efficiency solar cells is the issue of mobilities. Except for few special situations [44], the open circuit voltage and thus the LED quantum efficiency are independent of mobility. Thus, a low mobility is in no way an obstacle for the use of a material as LED. However, for solar cells, a low mobility leads to a low collection efficiency and photocurrent and thus is a big obstacle for high efficiencies.

To illustrate these differences, a brief look at our discrete two state device model is helpful. A low mobility is represented by a low coupling constant c of absorber and contact in this model. The open circuit situation is reached, when no current flows, i.e., when $c\nu = c\omega$. The open circuit voltage then follows from solving this equality for V as

$$V_{oc} = \frac{kT}{q} \ln\left(\frac{a\,\Delta\varphi}{a+b} + 1\right). \tag{81}$$

Obviously, V_{oc} does not depend on the coupling c to the contact but only on the radiative coupling a and non-radiative coupling b of the electrons to the photons and phonons. In contrast, the collection efficiency [see Eq. (62)] and in turn the quantum efficiency [see Eq. (64)] and the photocurrent depend on c and on a low mobility. Thus, the efficiency of a solar cell is sensitive to low mobilities via the photocurrent, while the LED quantum efficiency is in this simple model totally unaffected by mobilities.

6 The validity of the reciprocity relations

6.1 General considerations The principle of detailed balance relates the rates of any process to its inverse process in thermodynamic equilibrium. Although the equality of these rates holds only for equilibrium, the models based on detailed balance allow us to simulate also non-equilibrium situations [30]. However, the conclusions we derived from the detailed balance, i.e. the reciprocity theorems, depend on the linearity of the equations describing the system. In order to illustrate this claim, let us revisit the discrete, two state model. The validity of the Donolato-theorem [27] as well as the reciprocity between electroluminescence and quantum efficiency [28] relies on the fact, that collection efficiency and dark carrier concentration were both described by the same term

$$f_c = \frac{\Delta\nu_{dark}}{\omega - 1} = \frac{c}{a+b+c}. \tag{82}$$

As long as the *constants a, b*, and c are really constant, this equation holds. However, if they depend on illumination or voltage, the ratio $c/(a + b + c)$ will be different under illumination and short circuit conditions compared to the dark situation with applied voltage. Obvious examples where the validity of the reciprocity relations is not expected because of bias dependent rate constants are injection dependence of surface recombination [45] as well as tunneling at interfaces [46] or in the space charge region [47] where the rate constants are dependent on the applied voltage. At this point, we will not investigate these mechanisms any further but turn to the case of p–i–n-junctions.

6.2 p–i–n-junction solar cells In this type of devices departures from reciprocity are likely to appear already under practical working conditions without special mechanisms like tunneling. We perform numerical simulations using the software ASA [48] and compare voltage

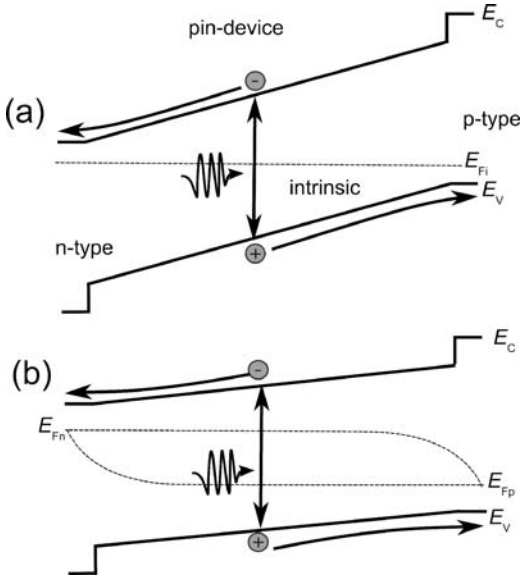

Figure 5 Scheme of a pin-junction solar cell in (a) short circuit and (b) under applied bias. Since the built-in field depends on voltage, the collection of photogenerated carriers may also depend on collection if mobilities are insufficiently high.

dependent and voltage independent collection and recombination. The p–i–n-type device is different from the p–n-type systems discussed up to now, since the boundary condition responsible for the application of a voltage is different. We have no longer a minority carrier contact from which minorities are injected according to the diode law (cf. Eq. (57)). Instead, the applied voltage changes the potential difference and the built in field between left and right contact.

As shown in Fig. 5a, under short circuit, there is a large potential difference and electric field in the device, leading to a better carrier collection. Under applied bias, the electric field decreases leading to a potentially voltage dependent collection of carriers. Thus, p–i–n-type devices have a built-in non-linearity in transport making them well suited for an investigation on the validity range of the reciprocity relations. A second property that distinguishes p–i–n-type devices from p–n-type devices is that minorities and majorities are not at all clearly defined. To understand the effect of electron and hole concentration being roughly equal, we have to look at the equation for the recombination rate. If we assume that the device is limited by non-radiative recombination via traps in the middle of the band gap, the recombination rate R follows from the Shockley-Read-Hall distribution as

$$R_{\mathrm{SRH}} = \frac{np - n_i^2}{(n + n_i)\,\tau_{\mathrm{p}} + (p + p_i)\,\tau_{\mathrm{n}}}, \tag{83}$$

where τ_{n} and τ_{p} are the lifetimes for electrons and holes. For a p-type material under low level injection, i.e. the typical situation in the bulk of a p–n-type solar cell, $n \ll p$ and $n_i \ll p$ holds and thus

$$R_{\mathrm{SRH}} = \frac{n}{\tau_{\mathrm{n}}} = \frac{n_0}{\tau_{\mathrm{n}}} \exp\left(\frac{qV}{kT}\right). \tag{84}$$

The recombination rate is hence proportional to the exponent of qV/kT, meaning that the system is linear. However, in general

$$R_{\mathrm{SRH}} \propto R_0(n, p)\, np \propto R_0(V) \exp(qV/kT), \tag{85}$$

holds. The voltage dependence of the prefactor R_0 vanishes if we can define minorities. Thus, we expect that the p–i–n-type solar shows several non-ideal features in collection and recombination.

Figure 6 shows the first simulations of (a) dark, (a,b) illuminated J/V, photocurrent $J_{\mathrm{ph}} = J_{\mathrm{d}} - J_{\mathrm{ill}}$, (c) electroluminescence spectrum ϕ_{em} and the quantum efficiencies $Q_{\mathrm{e,EL}}$ and $Q_{\mathrm{e,dir}}$. The parameters are a high mobility $\mu_{n,p} = 10^3\ \mathrm{cm^2(Vs)^{-1}}$ for electrons and holes, a direct re-

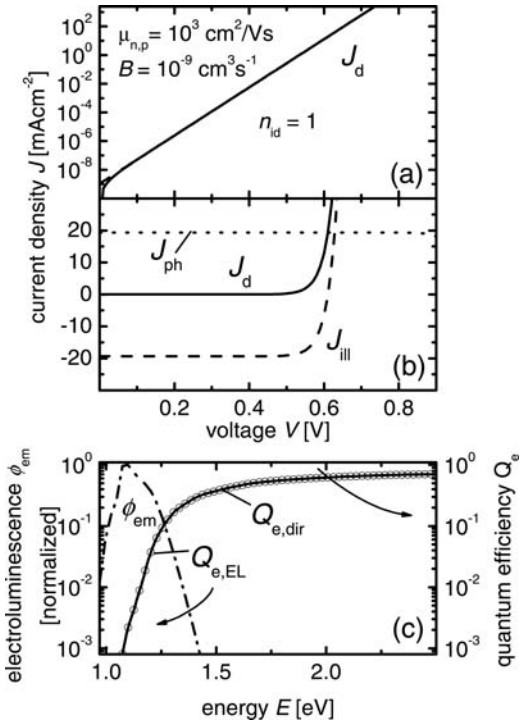

Figure 6 Comparison of the validity of three properties of photovoltaic devices: (a) ideality, (b) superposition and (c) optoelectronic reciprocity. Due to the choice of direct recombination and high mobilities, the diode ideality $n_{\mathrm{id}} = 1$ and the superposition principle (photocurrent $J_{\mathrm{ph}} = \mathrm{const}$) is valid as well as the optoelectronic reciprocity ($Q_{\mathrm{e,EL}} = Q_{\mathrm{e,dir}}$). The parameters chosen are the absorption coefficient of crystalline silicon, a thickness of 20 nm for p-type and n-type layer, an absorber thickness of 500 nm, a band gap of $E_{\mathrm{g}} = 1.12$ eV and effective density of states $N_{\mathrm{C}} = 2.81 \times 10^{19}\ \mathrm{cm^{-3}}$ and $N_{\mathrm{V}} = 2.88 \times 10^{19}\ \mathrm{cm^{-3}}$ of the conduction band and of the valence band and a doping concentration of $N_{\mathrm{A}} = N_{\mathrm{D}} = 10^{18}\ \mathrm{cm^{-3}}$ for the p-type and n-type region, respectively. These parameters are also used for Figs. 7–9.

combination coefficient $B = 10^{-9}$ cm^3 s^{-1}, a device thickness of $d = 500$ nm and an absorption coefficient α of crystalline silicon.

Figure 6a shows that the ideality of the dark current is unity. This is due to the assumption of direct recombination, where the recombination rate is given by $R_{dir} = Bnp$. Since B is a constant and independent of voltage and since np = const due to the high mobility, the recombination rate is proportional to exp (qV/kT), with an ideality of one.

Figure 6b shows that the photocurrent, i.e. the difference between the illuminated and dark J/V-curves is constant over voltage. That means that the superposition principle [49] is valid. Figure 6c shows that the quantum efficiency $Q_{e,EL}$ (circles) calculated from the EL spectrum (dash-dotted line) is equal to the directly measured $Q_{e,dir}$ (solid line). Thus, the optoelectronic reciprocity [Eq. (74)] is valid.

Figure 7 shows that for high mobilities, we can also use Shockley–Read–Hall (SRH) recombination and still obtain the same result for the superposition and the reciprocity, although the diode ideality differs from one.

This means that the recombination rate and thus the recombination current are voltage dependent and not proportional to exp (qV/kT). The voltage dependent recombination rate leads to a recombination current, which is described by $J_0(V)$ exp (qV/kT). The voltage dependent prefactor J_0 is equivalent to an ideality $n_{id} \neq 1$ [50]. Note here that the validity of the reciprocity for the high mobility limits shown in Figs. 6 and 7 is equivalent to the validity of Würfel's generalization [22] of Planck's and Kirchhoff's law.

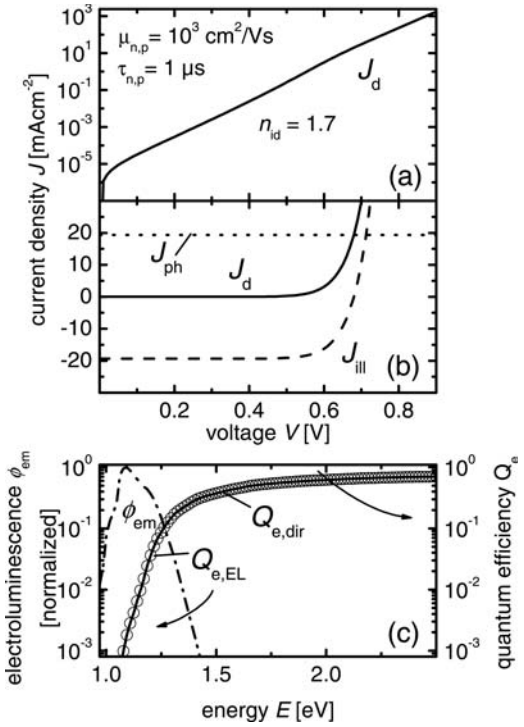

Figure 7 In spite of the choice of SRH-recombination leading to the diode ideality $n_{id} \approx 1.7$, the superposition principle (photocurrent J_{ph} = const) is valid as well as the optoelectronic reciprocity ($Q_{e,EL} = Q_{e,dir}$). This is due to the case that the mobilities are high, the quasi-Fermi levels are flat and thus the collection efficiency is practically unity for any position in the device. In this particular case, the validity of the optoelectronic reciprocity is trivial and equivalent to the validity of Würfel's generalization of Planck's and Kirchhoff's law.

Figure 8a shows that for direct recombination and low mobilities, the ideality of the dark current (solid line) starts to differ from one (dashed line) and the photocurrent becomes voltage dependent (see Fig. 8b). Now, also the optoelectronic reciprocity loses its validity ($Q_{e,EL} \neq Q_{e,dir}$) as shown in Fig. 8c. This is because collection and injection is now heavily field and thus voltage dependent and thus no longer the same in the illuminated short circuit situation and in the dark situation leading to the EL emission. The difference between $Q_{e,EL}$ and $Q_{e,dir}$ now depends on the bias conditions. For all simulations of $Q_{e,EL}$ we used $V = 0.6$ V. For higher voltages the built-in field becomes lower and thus the difference between the short circuit situation and the situation with applied bias becomes larger. For lower voltages $Q_{e,EL}$ and $Q_{e,dir}$ approach each other.

Figure 9a shows that for SRH-recombination and low mobilities the ideality of the dark current (solid line) is both higher than one and heavily voltage dependent just

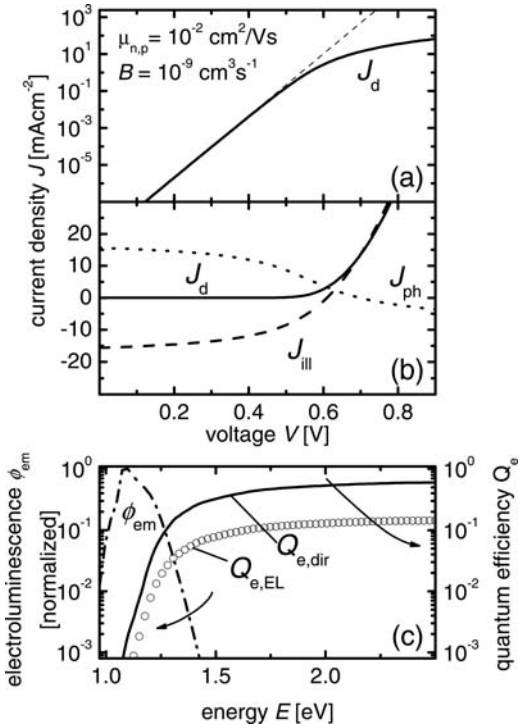

Figure 8 For direct recombination and low mobilities, (a) the ideality of the dark current (solid line) starts to differ from one (dashed line) and (b) the photocurrent becomes voltage dependent. Now, also the optoelectronic reciprocity loses its validity ($Q_{e,EL} \neq Q_{e,dir}$).

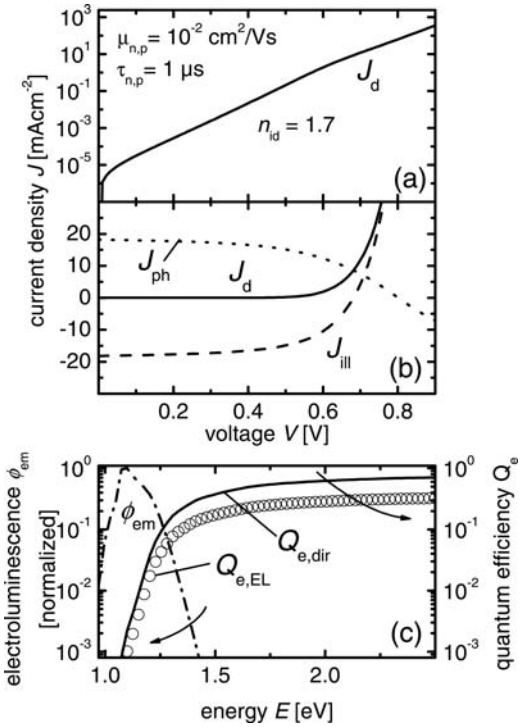

Figure 9 For SRH-recombination and low mobilities (a) the ideality of the dark current (solid line) is both higher than one and heavily voltage dependent just like (b) the photocurrent. The optoelectronic reciprocity loses its validity ($Q_{e,EL} \neq Q_{e,dir}$).

like (see Fig. 9b) the photocurrent. For the validity of the optoelectronic reciprocity the same conclusions apply as for Fig. 8, i.e. direct recombination with low mobilities: The voltage dependence of collection and injection leads to a difference between $Q_{e,EL}$ and $Q_{e,dir}$ depending on the applied voltage.

7 Conclusions The present paper reviews the numerous applications of the principle of detailed balance for the understanding of photovoltaic devices. The most prominent result of detailed balance is the Shockley–Queisser limit defining the efficiency limit of a solar cell by only considering incoming and outgoing photon fluxes, which are connected by detailed balance and thus define a thermodynamic limit for a given device. The device is only defined by its band gap and its temperature. How the device absorbs light and collects carriers is irrelevant for the Shockley–Queisser limit. However, applying the principle of detailed balance also to the internal, microscopic mechanisms of photovoltaic energy conversion allows us to derive three reciprocity relations connecting different working situations of a diode with each other. We show how the electroluminescence is connected to the photovoltaic quantum efficiency, how the dark carrier distribution is linked to the photocarrier collection (Donolato theorem) and how the open circuit voltage and the LED quantum efficiency depend on each other. Finally, we discuss the limits, both of the Shockley–Queisser theory and of the reciprocity. We show, how superposition, diode ideality and reciprocity behave in p–i–n-junction solar cells.

Acknowledgements We thank the German Federal Ministry of Education and Research (Nanovolt, 03SF0322H) and the German Research Foundation (Nanosun, RA 473/6-1) for partial funding of this project.

References

[1] D. Ginley, M. A. Green, and R. Collins, MRS Bull. **33**, 355 (2008).
[2] N. S. Lewis, Science **315**, 798 (2007).
[3] R. F. Service, Science **319**, 718 (2008).
[4] C. W. Tang, Appl. Phys. Lett. **48**, 183 (1986).
[5] G. Yu, J. Gao, J. C. Hummelen, F. Wudl, and A. J. Heeger, Science **270**, 1789 (1995).
[6] H. Hoppe and N. S. Sariciftci, J. Mater. Res. **19**, 1924 (2004).
[7] C. J. Brabec, N. S. Sariciftci, and J. C. Hummelen, Adv. Funct. Mater. **11**, 15 (2001).
[8] F. Yang, M. Shtein, and S. R. Forrest, Nature Mater. **4**, 37 (2005).
[9] P. W. M. Blom, V. D. Mihailetchi, L. J. A. Koster, and D. E. Markov, Adv. Mater. **19**, 1551 (2007).
[10] Y. Kim, S. Cook, S. M. Tuladhar, S. A. Choulis, J. Nelson, J. R. Durrant, D. D. C. Bradley, M. Giles, I. McCulloch, C.-S. Ha, and M. Ree, Nature Mater. **5**, 197 (2006).
[11] S. Bertho, G. Janssen, T. J. Cleij, B. Conings, W. Moons, A. Gadisa, J. D'Haen, E. Goovaerts, L. Lutsen, J. Manca, and D. Vanderzande, Sol. Energy Mater. Sol. Cells **92**, 753 (2008).
[12] J. Y. Kim, K. Lee, N. E. Coates, D. Moses, T.-Q. Nguyen, M. Dante, and A. J. Heeger, Science **317**, 222 (2007).
[13] B. O'Regan and M. Grätzel, Nature **353**, 737 (1991).
[14] M. Grätzel, Nature **414**, 338 (2001).
[15] P. Wang, S. M. Zakeeruddin, J. E. Moser, M. K. Nazeeruddin, T. Sekiguchi, and M. Grätzel, Nature Mater. **2**, 402 (2003).
[16] M. Law, L. E. Greene, J. C. Johnson, R. Saykally, and P. Yang, Nature Mater. **4**, 455 (2005).
[17] L. Schmidt-Mende, U. Bach, R. Humphry-Baker, T. Horiuchi, H. Miura, S. Ito, S. Uchida, and M. Grätzel, Adv. Mater. **17**, 813 (2005).
[18] J. Schrier, D. O. Demchenko, L.-W. Wang, and A. P. Alivisatos, Nano Lett. **7**, 2377 (2007).
[19] W. Shockley and H. J. Queisser, J. Appl. Phys. **32**, 510 (1961).
[20] M. A. Green, K. Emery, Y. Hishikawa, and W. Warta, Prog. Photovolt., Res. Appl. **16**, 61 (2008).
[21] M. Planck, Vorlesungen über die Theorie der Wärmestrahlung (Barth, Leipzig, 1906).
[22] P. Würfel, J. Phys. C, Solid State Phys. **15**, 3967 (1982).
[23] G. Kirchhoff, Ann. Phys. (Leipzig) **19**, 275 (1860).
[24] T. Tiedje, E. Yablonovitch, G. D. Cody, and B. G. Brooks, IEEE Trans. Electron Devices **31**, 711 (1984).
[25] U. Rau and J. H. Werner, Appl. Phys. Lett. **84**, 3735 (2004).
[26] U. Rau and R. Brendel, J. Appl. Phys. **84**, 6412 (1998).
[27] C. Donolato, Appl. Phys. Lett. **46**, 270 (1985).
[28] U. Rau, Phys. Rev. B **76**, 085303 (2007).

[29] M. A. Green, J. Appl. Phys. **81**, 268 (1997).
[30] T. Kirchartz and U. Rau, Thin Solid Films **516**, 7144 (2008).
[31] J. Mattheis, J. H. Werner, and U. Rau, Phys. Rev. B **77**, 085203 (2008).
[32] K. Misiakos and F. A. Lindholm, J. Appl. Phys. **58**, 4743 (1985).
[33] T. Markvart, IEEE Trans. Electron Devices **43**, 1034 (1996).
[34] W. van Roosbroeck and W. Shockley, Phys. Rev. **94**, 1558 (1954).
[35] T. Kirchartz and U. Rau, J. Appl. Phys. **102**, 104510 (2007).
[36] R. H. Friend, R. W. Gymer, A. B. Holmes, J. H. Burroughes, R. N. Marks, C. Taliani, D. D. C. Bradley, D. A. Dos Santos, J. L. Bredas, M. Logdlund, and W. R. Salaneck, Nature **397**, 121 (1999).
[37] C. Adachi, M. A. Baldo, S. R. Forrest, and M. E. Thompson, Appl. Phys. Lett. **77**, 904 (2000).
[38] J. Peet, J. Y. Kim, N. E. Coates, W. L. Ma, D. Moses, A. J. Heeger, and G. C. Bazan, Nature Mater. **6**, 497 (2007).
[39] J. Zhao, A. Wang, M. A. Green, and F. Ferrazza, Appl. Phys. Lett. **73**, 1991 (1998).
[40] M. A. Green, J. Zhao, A. Wang, P. J. Reece, and M. Gal, Nature **412**, 805 (2001).
[41] T. Kirchartz, U. Rau, M. Kurth, J. Mattheis, and J. H. Werner, Thin Solid Films **515**, 6238 (2007).
[42] T. Kirchartz, U. Rau, M. Hermle, A. W. Bett, A. Helbig, and J. H. Werner, Appl. Phys. Lett. **92**, 123502 (2008).
[43] G. Dennler, M. C. Scharber, and C. J. Brabec, Adv. Mater., submitted (2008).
[44] T. Kirchartz, B. E. Pieters, K. Taretto, and U. Rau, J. Appl. Phys., in print (2008); DOI: 10.1063/1.3013904.
[45] A. G. Aberle, J. Schmidt, and R. Brendel, J. Appl. Phys. **79**, 1491 (1996).
[46] F. A. Padovani and R. Stratton, Solid-State Electron. **9**, 695 (1966).
[47] U. Rau, Appl. Phys. Lett. **74**, 111 (1999).
[48] M. Zeman, J. van den Heuvel, B. E. Pieters, M. Kroon, and J. Willemen, Advanced Semiconductor Analysis (TU Delft, 2003).
[49] S. J. Robinson, A. G. Aberle, and M. A. Green, J. Appl. Phys. **76**, 7920 (1994).
[50] P. J. Rostan, U. Rau, V. X. Nguyen, T. Kirchartz, M. B. Schubert, and J. H. Werner, Sol. Energy Mater. Sol. Cells **90**, 1345 (2006).